Field-modulated thermopower in $SrTiO_3$-based field-effect transistors with amorphous $12CaO \cdot 7Al_2O_3$ glass gate insulator

Hiromichi Ohta,[1,a] Yumi Masuoka,[2] Ryoji Asahi,[2] Takeharu Kato,[3] Yuichi Ikuhara,[3,4] Kenji Nomura,[5] and Hideo Hosono[5,6]

[1]*Graduate School of Engineering, Nagoya University, Furo-cho, Chikusa, Nagoya 464-8603, Japan and PRESTO, Japan Science and Technology Agency, Honcho, Kawaguchi 332-0012, Japan*
[2]*Toyota Central R&D Laboratories, Nagakute, Aichi-gun 480-1192, Japan*
[3]*Japan Fine Ceramics Center, 2-4-1 Mutsuno, Atsuta, Nagoya 456-8587, Japan*
[4]*Institute of Engineering Innovation, The University of Tokyo, 2-11-16 Yayoi, Bunkyo, Tokyo 113-8656, Japan*
[5]*ERATO-SORST, Japan Science and Technology Agency, Tokyo Institute of Technology, 4259 Nagatsuta, Midori, Yokohama 226-8503, Japan*
[6]*Frontier Research Center, Tokyo Institute of Technology, 4259 Nagatsuta, Midori, Yokohama 226-8503, Japan*

(Received 2 August 2009; accepted 27 August 2009; published online 18 September 2009)

We report transistor characteristics and field-modulated thermopower (S) for single crystal $SrTiO_3$-based field-effect transistors (FETs). We use 150-nm-thick amorphous $12CaO \cdot 7Al_2O_3$ glass as the gate insulator of the $SrTiO_3$-FET. The resulting $SrTiO_3$-FET exhibits excellent transistor characteristics at room temperature: on-to-off current ratio greater than 10^6, threshold gate voltage of +1.1 V, subthreshold swing of approximately 0.3 V $decade^{-1}$, and effective mobility of 2 $cm^2 V^{-1} s^{-1}$. The field-modulated S-value of the $SrTiO_3$-FET varied from −900 to −580 $\mu V K^{-1}$ with electric fields of up to 2 MV cm^{-1}, demonstrating the effectiveness of the FET structure for the exploration of thermoelectric materials. © *2009 American Institute of Physics*.
[doi:10.1063/1.3231873]

Thermoelectric (TE) energy conversion technology has attracted a great deal of attention for converting waste heat into electricity by utilizing the Seebeck effect, as well as for refrigerating various devices by means of the Peltier effect.[1] The performance of thermoelectric materials is evaluated in terms of a dimensionless figure of merit ZT, given by $ZT = S^2 \cdot \sigma \cdot T \cdot \kappa^{-1}$, where T, S, σ, and κ are, the absolute temperature, the thermopower, and electrical and thermal conductivities, respectively. Today, TE materials with $ZT > 1$, which is necessary for practical applications, are being rigorously explored, mostly using charge carrier-doped semiconductors with various doping levels. Consequently, a great deal of material is needed to optimize TE properties.

A field-effect transistor (FET) structure on single-crystalline materials, however, would be a powerful tool in exploring TE materials because it provides the charge carrier dependence of both S and σ values simultaneously.[2] In this letter, we focus on $SrTiO_3$ to demonstrate the effectiveness of an FET structure for exploring TE materials. $SrTiO_3$ has attracted much attention as an n-type TE material due to its potential advantages over heavy metallic alloys such as Bi_2Te_3 and PbTe in chemical and thermal robustness.[3]

In order to unequivocally measure the field-modulated S values, $SrTiO_3$-FETs with excellent transistor characteristics are required. Although several attempts toward the realization of $SrTiO_3$-FETs have been made and several gate insulators including MgO,[4] amorphous (a-)Al_2O_3,[5] $CaHfO_3$,[6,7] and parylene[8] have been proposed to date, it is still difficult to fabricate $SrTiO_3$-FET with excellent transistor characteristics. For example, in our preliminary study, we first chose a-Al_2O_3 as gate insulator because it can be deposited without any substrate heating using the pulsed laser deposition (PLD) process, which may minimize damage layer formation on the $SrTiO_3$ surface. However, several grain structures were observed in an atomic force microscope (AFM) image of the resulting 200-nm-thick a-Al_2O_3 film, which could cause relatively large gate leakage current. Furthermore, some of the transistor characteristics such as effective mobility (μ_{eff}) and subthreshold swing (S factor) were unsatisfactory, μ_{eff} ~0.6 $cm^2 V^{-1} s^{-1}$ and S factor ~2.4 V $decade^{-1}$ (data not shown).

We then tested various gate insulator materials to obtain $SrTiO_3$-FETs with superior transistor characteristics and found a-$12CaO \cdot 7Al_2O_3$ (Refs. 9–11) (a-C12A7, dielectric constant $\varepsilon_r = 12$) to be an excellent gate insulator for $SrTiO_3$.[12] The $SrTiO_3$-FET exhibits excellent transistor characteristics at room temperature: on-to-off current ratio $> 10^6$, threshold gate voltage +1.1 V, subthreshold swing ~0.3 V $decade^{-1}$, and effective mobility ~2 $cm^2 V^{-1} s^{-1}$. By applying a gate electric field of up to +2 MV cm^{-1}, the thermopower of the $SrTiO_3$-FET was modulated from −900 to −580 $\mu V K^{-1}$.

Schematic device structure and a photograph of the $SrTiO_3$-FET are shown in Fig. 1. First, 20-nm-thick metallic Ti films, used as the source and drain electrodes, were deposited through a stencil mask by electron beam (EB) evaporation (base pressure ~10^{-4} Pa, no substrate heating) onto a stepped $SrTiO_3$ substrate ($10 \times 10 \times 0.5$ mm^3), treated with NH_4F-buffered HF solution.[13] Second, 150-nm-thick a-C12A7 film was deposited through a stencil mask by PLD (KrF excimer laser, fluence ~3 J cm^{-2} $pulse^{-1}$, oxygen pressure ~0.1 Pa) using dense polycrystalline C12A7 ceramic as target. Finally, 20-nm-thick metallic Ti films, used as the

[a]Author to whom correspondence should be addressed. Electronic mail: h-ohta@apchem.nagoya-u.ac.jp.

 © 2009 American Institute of Physics

Downloaded 15 Sep 2010 to 133.6.32.9. Redistribution subject to AIP license or copyright; see http://apl.aip.org/about/rights_and_permissions

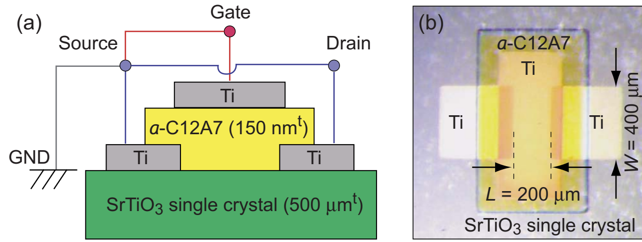

FIG. 1. (Color online) (a) Schematic device structure and (b) photograph of the $SrTiO_3$-FET. Ti films (20 nm thick) are used as the source, drain, and gate electrodes. A 150-nm-thick *a*-C12A7 film is used as the gate insulator. Channel length (L) and channel width (W) are 200 and 400 μm, respectively.

gate electrode, was deposited through a stencil mask by EB evaporation. After the deposition processes, the devices were annealed at 200 °C for 30 min in air to reduce the off current.

Halo peaking only at $2\theta \sim 30°$ was observed in the glancing incidence x-ray diffraction (XRD) pattern of the resulting C12A7 film (Cu $K\alpha_1$, x-ray angle of incidence 0.5°) [Fig. 2(a)]. This pattern was very similar to the halo pattern of the C12A7 glass.[11] The density of the C12A7 film was ~2.9 g cm^{-3} as evaluated by grazing incidence x-ray reflectivity (GIXR, ATX-G, Rigaku Co., data not shown) and was in a good correspondence with that of C12A7 glass (2.92 g cm^{-3}).[11] It should be noted that any grain structure in the as-deposited film was not observed in the topographic AFM image [Fig. 2(a) inset]. Furthermore, no grain structure was observed in the cross sectional high-resolution transmis-

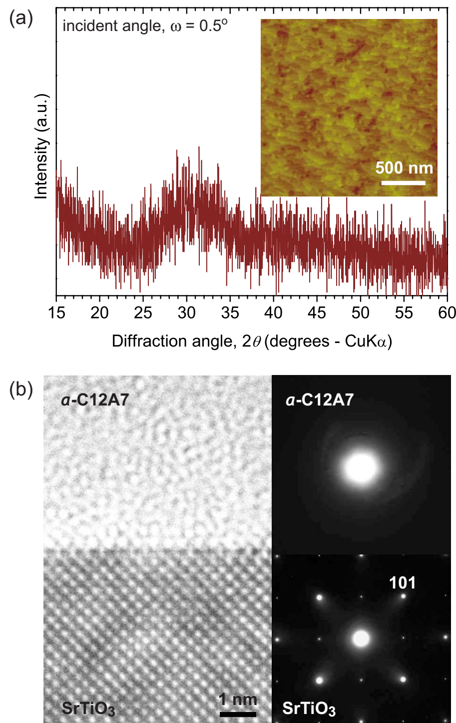

FIG. 2. (Color online) (a) Glancing angle XRD pattern of a 150-nm-thick *a*-C12A7 layer. Broad halo of *a*-C12A7 is seen around $2\theta \sim 30°$. Topographic AFM image (2×2 μm^2) of the C12A7 film on the $SrTiO_3$ surface is also shown in the inset. (b) Cross-sectional HRTEM image of the 150-nm-thick *a*-C12A7/$SrTiO_3$ heterointerface, showing an abrupt interface of *a*-C12A7/$SrTiO_3$. Featureless image of *a*-C12A7 clearly indicates that the *a*-C12A7 layer is glass. A broad halo pattern is seen in the selected area electron diffraction patterns of *a*-C12A7 (right).

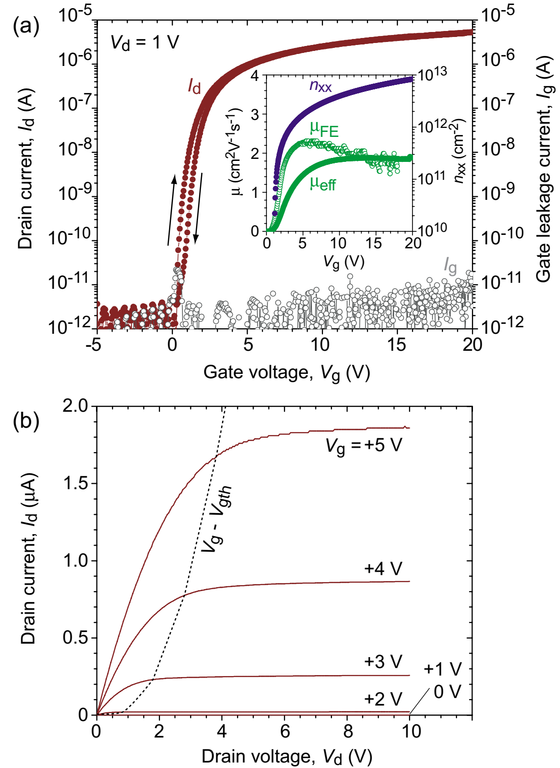

FIG. 3. (Color online) (a) Typical transfer and (b) output characteristics of the $SrTiO_3$-FET with 150-nm thick *a*-C12A7 ($\varepsilon_r = 12$) gate insulator at room temperature. Channel length (L) and channel width (W) are 200 and 400 μm, respectively. Effective mobility (μ_{eff}), field-effect mobility (μ_{FE}) and sheet charge density (n_{xx}) vs V_g plots for the $SrTiO_3$-FET are also shown in the inset of (a). The dotted line in (b) indicates $V_g - V_{gth}$ value.

sion electron microscope (HRTEM) image of the *a*-C12A7/$SrTiO_3$ interface region (TOPCON EM-002B, acceleration voltage of 200 kV, TOPCON) [Fig. 2(b)]. A broad halo pattern is seen in the selected area electron diffraction patterns of *a*-C12A7. We thus concluded that the deposited film was *a*-C12A7 glass.

Transistor characteristics of the resultant FETs were measured by using a semiconductor device analyzer (B1500A, Agilent) at room temperature in air. Figure 3 shows typical (a) transfer and (b) output characteristics of the resultant FET. Drain current (I_d) of the FET increased markedly as the gate voltage (V_g) increased, hence the channel was *n*-type, and electron carriers were accumulated by positive V_g [Fig. 3(a)]. A small hysteresis (~0.5 V) in I_d, probably due to traps (mid-10^{11} cm^{-2}) at the *a*-C12A7/$SrTiO_3$ interface, was also seen [Fig. 3(a)]. We observed a clear pinch-off and saturation in I_d [Fig. 3(b)], indicating that the operation of this FET conformed to standard FET theory. The on-to-off current ratio, *S*-factor, and threshold gate voltage (V_{gth}), which were obtained from a linear fit of an $I_d^{0.5} - V_g$ plot (data not shown), are $>10^6$, ~0.3 V $decade^{-1}$ and +1.1 V, respectively. We calculated the effective mobility (μ_{eff}) of the $SrTiO_3$-FETs from $\mu_{eff} = (e \cdot n_{xx} \cdot R_{xx})^{-1}$, where e, n_{xx}, and R_{xx} were elementary charge, sheet charge concentration and sheet resistance, respectively. The n_{xx} values were obtained from $n_{xx} = C_i(V_g - V_{gth})$, where C_i was the capacitance per unit area (71 nF cm^{-2}) [Fig. 3(a) inset]. We noted μ_{eff} of the FET increases drastically with V_g and reaches at ~2 cm^2 V^{-1} s^{-1}, which is ~30% of the room temperature

Downloaded 15 Sep 2010 to 133.6.32.9. Redistribution subject to AIP license or copyright; see http://apl.aip.org/about/rights_and_permissions

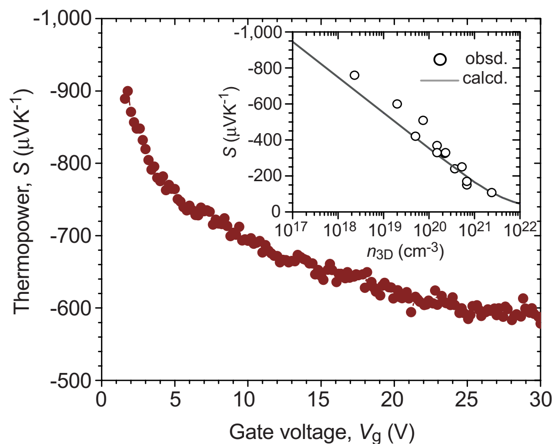

FIG. 4. (Color online) Field-modulated thermopower (S) for the $SrTiO_3$-FET channel. $S-n_{3D}$ (log scaled) plots (Ref. 14) for electron doped $SrTiO_3$ are also shown in the inset as a reference.

Hall mobility of electron-doped $SrTiO_3$ (μ_{Hall} ~ 6 cm^2 V^{-1} s^{-1}) [Fig. 3(a) inset].

We measured field-modulated thermopower (S) of the $SrTiO_3$-FET as follows. First, a temperature difference (ΔT $=0.2-1.5$ K) was introduced between the source and drain electrodes by using two Peltier devices. Then, thermoelectromotive force (V_{TEMF}) was measured during the V_g sweeping. The values of S were obtained from the slope of V_{TEMF} $-\Delta T$ plots (data not shown). Figure 4 shows $S-V_g$ plots for the $SrTiO_3$-FET. The S values are negative, confirming that the channel is n-type. The $|S|$ value gradually decreases from 900 to 580 μV K^{-1}, which corresponds to an increase of the volume charge density (n_{3D}) from $\sim 2\times 10^{17}$ to ~ 8 $\times 10^{18}$ cm^{-3} (see Fig. 4 inset[14]), due to the fact that electron carriers are accumulated by positive V_g (up to +30 V).

In summary, we have shown transistor characteristics and field-modulated thermopower S of the $SrTiO_3$-based FET. The $SrTiO_3$-FET with 150-nm-thick amorphous $12CaO\cdot 7Al_2O_3$ (ε_r=12) gate insulator exhibits excellent transistor characteristics at room temperature: on-to-off current ratio $>10^6$, threshold gate voltage +1.1 V, subthreshold swing ~ 0.3 V $decade^{-1}$, and effective mobility ~ 2 cm^2 V^{-1} s^{-1}. While the electric field was increased of up to 2 MV cm^{-1}, S was clearly modulated from -900 to -580 μV K^{-1}, demonstrating that the FET structure was indeed effective for the exploration of thermoelectric materials.

The authors would like to thank D. Kurita, S. Nakagawa, A. Yoshikawa, K. Uchida, and K. Koumoto for their valuable discussions and experimental help. A part of this work was financially supported by MEXT (Nano Materials Science for Atomic-scale Modification, Grant No. 20047007).

[1] F. J. DiSalvo, Science **285**, 703 (1999).
[2] W. Liang, A. I. Hochbaum, M. Fardy, O. Rabin, M. Zhang, and P. Yang, Nano Lett. **9**, 1689 (2009).
[3] H. Ohta, Mater. Today **10**, 44 (2007), and references therein.
[4] I. Pallecchi, G. Grassano, D. Marrié, L. Pellegrino, M. Putti, and A. S. Siri, Appl. Phys. Lett. **78**, 2244 (2001).
[5] K. Ueno, I. H. Inoue, H. Akoh, M. Kawasaki, Y. Tokura, and H. Takagi, Appl. Phys. Lett. **83**, 1755 (2003).
[6] K. Shibuya, T. Ohnishi, T. Uozumi, T. Sato, M. Lippmaa, M. Kawasaki, K. Nakajima, T. Chikyow, and H. Koinuma, Appl. Phys. Lett. **88**, 212116 (2006).
[7] K. Shibuya, T. Ohnishi, M. Lippmaa, M. Kawasaki, and H. Koinuma, Appl. Phys. Lett. **85**, 425 (2004).
[8] H. Nakamura, H. Takagi, I. H. Inoue, Y. Takahashi, T. Hasegawa, and Y. Tokura, Appl. Phys. Lett. **89**, 133504 (2006).
[9] K. Hayashi, S. Matsuishi, T. Kamiya, M. Hirano, and H. Hosono, Nature (London) **419**, 462 (2002).
[10] S. Watauchi, I. Tanaka, K. Hayashi, M. Hirano, and H. Hosono, J. Cryst. Growth **237**, 801 (2002).
[11] S.-W. Kim, Y. Toda, K. Hayashi, M. Hirano, and H. Hosono, Chem. Mater. **18**, 1938 (2006).
[12] In our preliminary experiments, the dielectric constant (ε_r) of a-C12A7 was determined to ~ 12, which was measured using a Ti/a-C12A7/Ti capacitor deposited on $SrTiO_3$ substrate by a precision LCR meter (Model 4284A, Agilent). Typical breakdown field of the a-C12A7 film was ~ 3 MV cm^{-1}, which corresponds to $n_{xx}\sim 2\times 10^{13}$ cm^{-2}. The breakdown behavior of a-C12A7 is similar to that of PLD-deposited a-Al_2O_3 and a-$LaAlO_3$; S. Yaginuma, J. Yamaguchi, K. Itaka, and H. Koinuma, Thin Solid Films **486**, 218 (2005).
[13] M. Kawasaki, K. Takahashi, T. Maeda, R. Tsuchiya, M. Shinohara, O. Ishiyama, T. Yonezawa, M. Yoshimoto, and H. Koinuma, Science **266**, 1540 (1994).
[14] H. Ohta, K. Sugiura, and K. Koumoto, Inorg. Chem. **47**, 8429 (2008).

Downloaded 15 Sep 2010 to 133.6.32.9. Redistribution subject to AIP license or copyright; see http://apl.aip.org/about/rights_and_permissions